Proceedings of the 7th International Conference on HydroScience and Engineering

Philadelphia, USA September 10-13, 2006 (ICHE 2006)

ISBN: 0977447405

Drexel University

College of Engineering

ON THE INITIATION OF MEANDERING AND THE SUBSEQUENT PLAN-DEVELOPMENT OF MEANDER LOOPS

Ana Maria Ferreira da Silva[1]

ABSTRACT

The formation and the different plan arrangements of large-scale horizontal coherent structures in river flows are discussed on the basis of recent turbulence studies and all available morphological data. It is shown that the wavelength of a meandering flow coincides with the length of the (basic) one-row configuration of turbulence coherent structures at the beginning of "experiment" (at time $t = 0$, when the channel is still straight). The initiation of meandering is attributed to the action on the movable banks of the sequence of these structures, either by their direct impact on the banks or by the convective action of the internal meandering they generate. The subsequent time-development of the so-initiated meandering and the eventual fate of a meandering stream are explained by invoking the regime-trend. The considerations in this paper are used to derive the prediction criteria for the meandering of initially straight and wide streams in cohesionless alluvium. The paper concludes with the introduction of a method for the determination of the stable plan shape of a meandering course.

1. INTRODUCTION

Why do some rivers meander, while others remain straight or braid? Why do some meandering rivers continually tend to expand their meander loops, while others acquire a reasonably stable plan-configuration? And what are the criteria needed to predict whether a stream will meander or not, and if yes, how much it will meander?

This paper intends to answer these questions by resorting to the large-scale horizontal turbulence and the regime-trend. It is assumed throughout this text that the "experiment" commences, at time $t = 0$, in a trapezoidal wide initial channel ($B/h > \approx 15$, say): the stream is embedded in cohesionless alluvium, the stream bed and banks thus being movable; the initial turbulent flow is uniform.

Following Tison (1949), it is generally accepted that no periodic alluvial forms (bed or plan forms) occur in a laminar flow (see e.g. Velikanov 1955, 1958 and Yalin 1977). Therefore a hypothesis aiming to explain the origin of periodic alluvial forms must have a meaning only if the flow is turbulent. Many prominent earlier researchers, including Matthes (1947), Velikanov (1955), Grishanin (1979), Kondratiev et al. (1982), etc., hinted on associations between large-scale turbulence and the occurrence of various alluvial forms, and especially bed forms. However, such associations could not be elaborated in any satisfactory way before the relatively recent discovery of

[1] Associate Professor, Department of Civil Engineering, Queen's University, Kingston, Ontario, Canada K7L 3N6 (amsilva@civil.queensu.ca)

turbulence coherent structures and bursting processes. Jackson (1976) and Yalin (1977) appear to have been the first to realize the river morphodynamic implications of bursting processes. Yalin (1992) noted that the average dune length $(\approx 6h)$ is approximately equal to the largest dimension of the coherent structures (bursts) of vertical macroturbulence, and used this fact to produce a detailed theory explaining the formation of dunes by vertical bursts. Just like dunes can be attributed to the vertical macroturbulence of the flow, it seems likely that alternate bars and meandering – whose length and wavelength, respectively, are proportional to the flow width B – stem from the horizontal macroturbulence of the flow (as apparently first suggested by Yalin 1977, Kishi 1980 and Jaeggi 1984). The first aim of this paper is to explore this conjecture by considering available flow and morphological data in the light of recent discoveries in turbulence.

In the recent literature, meandering is also often associated with the regime-trend. A second aim of this paper is to clarify the different roles played by turbulence and the regime-trend on the meandering process.

The paper is to be viewed as an updated summary of material on the topic presented by da Silva (1991), Yalin (1992), and Yalin and da Silva (2001).

2. VERTICAL AND HORIZONTAL TURBULENCE STRUCTURES

Following Hussain (1983), the term "coherent structure" (CS) is used here to designate the largest conglomeration of turbulent eddies which has a prevailing sense of rotation, the term burst, to designate the evolution of a CS during its life-span T. The bursts can be vertical (V) or horizontal (H). The CS's of the former rotate in the $(x;z)$-planes, those of the latter, in the $(x;y)$-planes (Figure 1).

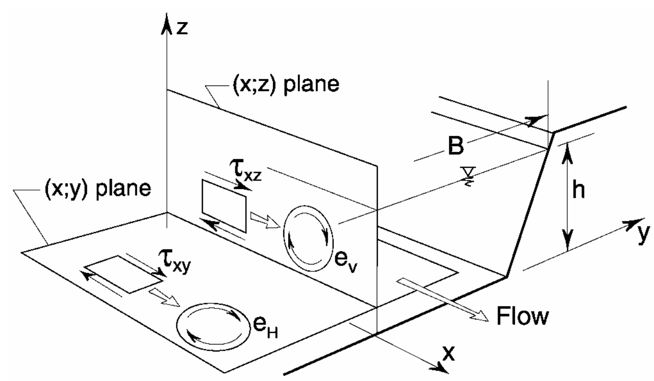

Figure 1 Vertical and horizontal planes of rotation of CS's

It is not yet known how exactly the aforementioned CS's originate and develop, and the following is a brief "synthesis" of the contents of Blackwelder (1978), Grishanin (1979), Cantwell (1981), Hussain (1983), Gad-el-Hak and Hussain (1986), Rashidi and Banerjee (1988), and several others.

i) A vertical burst-forming CS originates at a location around a point P (at O_i; see Figure 2(a)) near the flow boundary. At $t = 0$, a future macroturbulent eddy e_V ("transverse vortex") rolls-up at P (which is assumed to be at $x = 0$), and it is ejected, together with the fluid under it, away from the bed. This total fluid mass moves towards the free surface, as it is conveyed by the flow downstream (*ejection phase*). In the process, the moving fluid mass continually enlarges (by engulfment) and new eddies e'_V, e''_V, …, are generated (by induction) – thus a continually growing CS comes into being. When this structure becomes as large as to touch the free surface, it disintegrates (*break-up* *phase*) into a multitude of smaller and then even smaller eddies … until their size becomes as small as the lower limit ν / v_*, where their energy is dissipated (as implied by the "Eddy-Cascade Theory"). The neutralized fluid mass then moves downstream – towards the bed (*sweep stage*), with a substantially smaller velocity than that of ejection. At $t = T_V$, the fluid arrives at $x = \lambda_V$, which prompts the initiation of the "new" cycle at the next downstream point *P* (Hussain 1983, Nezu and Nakagawa 1993, etc.). The above described cycle is referred to as *burst-cycle*, or simply, as *burst*.

The conceptual Figure 2(a) shows (in a stationary frame) a *V*-burst cycle of an open-channel flow; the cine-record in Figure 2(b) shows (in a convective frame) an instantaneous view of two consecutive CS's.

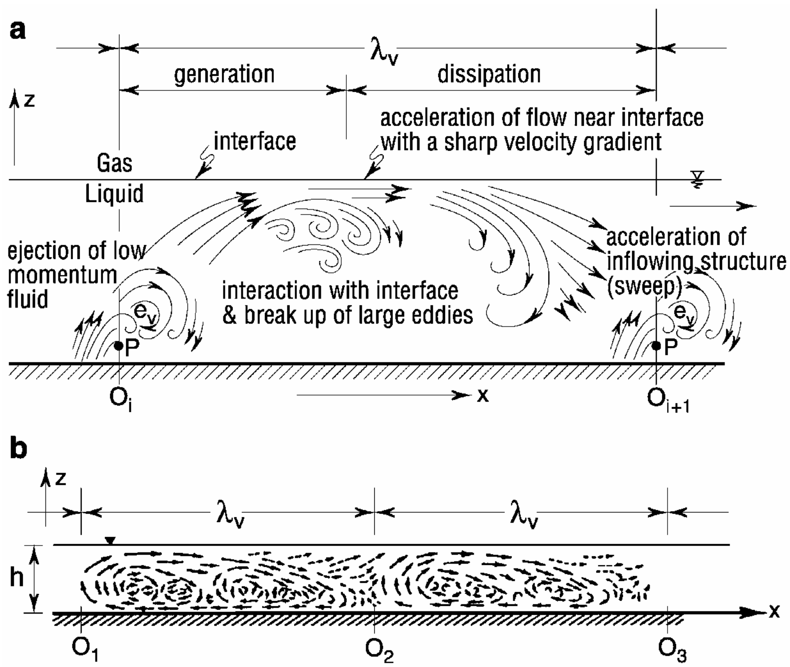

Figure 2 (a) Conceptual representation of a *V*-burst cycle (after Rashidi and Banerjee 1988); (b) Cine-record showing an instantaneous view of two consecutive CS's (from Klaven 1966)

ii) The analogous is valid, *mutatis mutandi*, for an *H*-burst. The difference appears to be in the length scale: all "lengths" of the large-scale vertical turbulence are proportional to the flow depth *h*; those of the large-scale horizontal turbulence, to the flow width *B*. The burst-forming HCS's extend (along z) throughout the flow thickness h, and they can thus be likened to thin horizontal "disks" (Yokosi 1967).

The HCS's originate at the points O_i near the banks (see Figure 5(a)) and the free surface, where horizontal shear stresses τ_{xy} are the largest. Afterwards, they are conveyed by the mean flow downstream, while growing in size. Provided that the width-to-depth ratio is not too "large" (see Section 3.2), then the HCS's will grow until their lateral extent becomes as large as *B*. At this point, they interact with the opposite bank and disintegrate. The neutralized fluid mass returns to its original bank so as to arrive there at $t = T_H$. It is likely that if the bursts are "fired" from the points O_1, O_2, … at the times $t = 0$, 1, 2, …, say, then at the points O_1', O_2', … they are "fired" at $t = 1/2$, $3/2$, … (see da Silva 1991).

iii) The burst lengths λ_V and λ_H are found to be independent of the inner variables $v_* k_s / \nu$ and k_s / h: they scale, respectively, with the outer variables h and B (see e.g. Nezu and Nakagawa 1993, Gad-el-Hak and Hussain 1986, Cantwell 1981). Indeed, as can be noted e.g. from the plots of measured (by various authors) values of λ_V / h versus flow Reynolds number Re in Figures 2.4(a) and (b) in Yalin and da Silva (2001), the data-points of λ_V / h cluster at the level ≈ 6, irrespective of what the value of $\mathrm{Re} = u_{av} h / \nu \ (= c(h/k_s)(v_* k_s / \nu))$ might be. Thus

$$\frac{\lambda_V}{h} \approx 6 \tag{1}$$

(see also Roy et al. 2004). Similarly, the oscillograms of flow velocity recorded by Yokosi (1967) in Uji River, Japan, and those obtained by Dementiev (1962) in Syr-Darya River, former U.S.S.R. (and reproduced in Figures 3.15 and 3.16 in da Silva 1991 and Figures 2.18 to 2.20 in Yalin 1992) indicate that the dimensionless λ_H, viz λ_H / B, can also be expressed as

$$\frac{\lambda_H}{B} \approx 6\,. \tag{2}$$

3. MORPHOLOGICAL CONSEQUENCES OF VERTICAL AND HORIZONTAL TURBULENCE STRUCTURES

3.1 Dunes and Alternate Bars

The superimposition of the sequence of coherent structures on the basic flow must render the flow to acquire a sequence of periodic (along x and t) non-uniformities, with the straight and parallel streamlines deforming into periodically undulated (wave-like) ones. The resulting wave-like streamlines must in turn, by virtue of the sediment transport continuity equation, lead to the emergence of the periodic (along x) bed- and/or bank-forms (j) (see more on the topic in Yalin and da Silva 2001). These initial forms must grow with the passage of time (by coalescence) until they acquire their developed length Λ_j that is the same as the burst length:

$$\Lambda_j = \lambda_V \ \text{ or } \ \lambda_H\,. \tag{3}$$

i) Yalin (1977) (see also Yalin 1992) has shown that if the uniform initial flow can be treated as two-dimensional, then the length Λ_d of the developed dunes produced by this flow can be expressed as

$$\frac{\Lambda_d}{h} \approx 6 \cdot \phi_d(X, Z). \tag{4}$$

From the experimental family of curves implying eq. 4 (Figure 7.28 in Yalin 1977 or Figure 2.8 in Yalin and da Silva 2001), it is clear that if the initial flow is rough turbulent, i.e. if $v_* k_s / \nu \approx 2X >\approx 70$, then $\phi_d(X, Z) \to \approx 1$ and eq. 4 becomes

$$\frac{\Lambda_d}{h} \approx 6\,. \tag{5}$$

The fact that the Λ_d-relation (5) is in remarkable coincidence with the λ_V-relation (1) strongly suggests that dunes are the “imprints” of vertical coherent structures on the deformeable surface of a mobile bed (see Figure 3), as apparently first proposed by Yalin (1977). A detailed description of dune formation by vertical bursts is given by Yalin (1992).

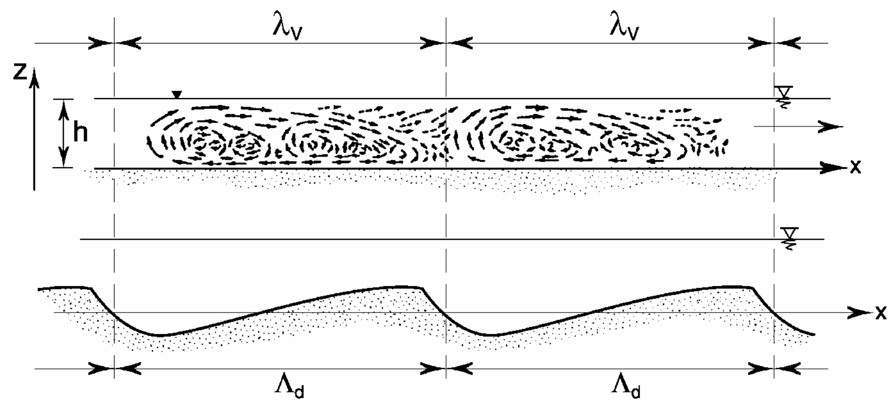

Figure 3 Longitudinal view of sequences of VCS's and of dunes

ii) Consider now the case of alternate bars. The numerous data available for these bed forms indicate that the average alternate bar length Λ_a is proportional to the flow width (see e.g. Figures 4(a) and (b)).

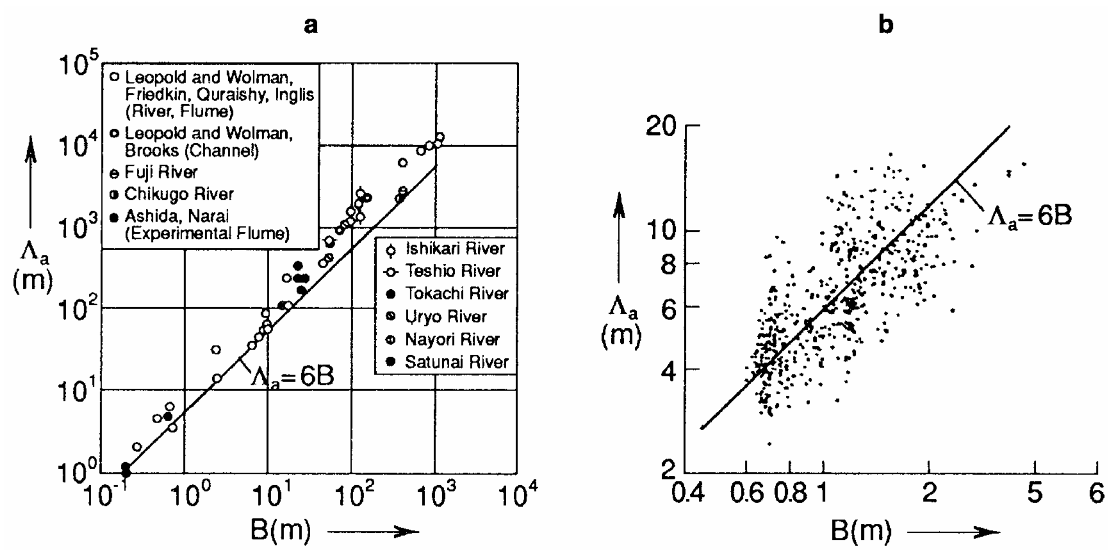

Figure 4 Plots of measured alternate bar length versus flow width. a) from JSCE (1973); b) from Hayashi (1971)

The current practice is to express the dimensionless (average) alternate bar length as

$$\frac{\Lambda_a}{B} \approx 6\,. \tag{6}$$

The similarity between the expressions of dune length and alternate bar length (eqs. 5 and 6) is striking. Since h and B are vertical and horizontal dimensions, respectively, the expression 6 can be viewed as the horizontal counterpart of the expression 5. This in itself suggests that if dunes are caused by a certain mechanism inherent in vertical turbulence, then alternate bars should be due to analogous mechanism inherent in vertical turbulence. The possibility that alternate bars are but the "horizontal version" of dunes appears to have been suggested first by Kishi (1980) and Jaeggi (1984): no coherent structures are mentioned, however, by these authors. In the light of the present understanding on turbulence coherent structures, the coincidence between the average horizontal burst length and the average alternate bar length (as implied by the relations 2 and 6) cannot but be viewed as a strong indication that alternate bars are very likely merely the "imprints" on the surface of a mobile bed of horizontal coherent structures (see Figure 5).

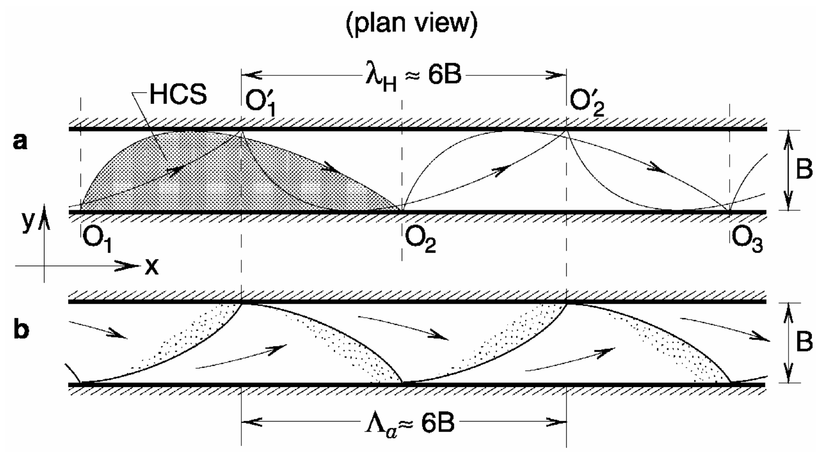

Figure 5 (a) Plan view of sequences of HCS's; (b) Plan view of alternate bars

3.2 Different Configurations of Horizontal Coherent Structures and Their Morphological Implications

If the relative flow width is too large, then the horizontal bursts emitted from one bank must not be expected to be able to grow as to reach the opposite bank, for they will be destroyed before that by friction. In this case, the horizontal coherent structures issued from both banks may meet each other in the midst of the stream, or even not be able to meet at all. Thus instead of the (basic) one-row burst configuration and single-row bars (i.e. alternate bars), the further increment of the relative flow width will lead to 2-row burst configuration and 2-row bars, 3-row burst configuration and 3-row bars, …, n-row burst configuration and n-row bars (see Figure 6).

The length of the n-row bars (Λ_n) is given by $\Lambda_n \approx 6B/n$ (Muramoto and Fujita 1978, Ikeda 1983, 1984, Fujita and Muramoto 1989). Therefore the length of n-row bursts must be expected to be given by

$$(\lambda_H)_n = \Lambda_n \approx \frac{6B}{n} \qquad \text{(where } n = 1,2,3,..., \text{ and } \Lambda_1 \text{ implies } \Lambda_a\text{).} \qquad (7)$$

No attempt has been made to date to measure $(\lambda_H)_n$ for $n \geq 2$.

4. INITIATION OF MEANDERING

4.1 Geometric Characteristics of Meandering Streams

Before proceeding further, the following pertinent aspects of the geometry of meandering streams – invoked in the remaining sections of the paper – should be mentioned.

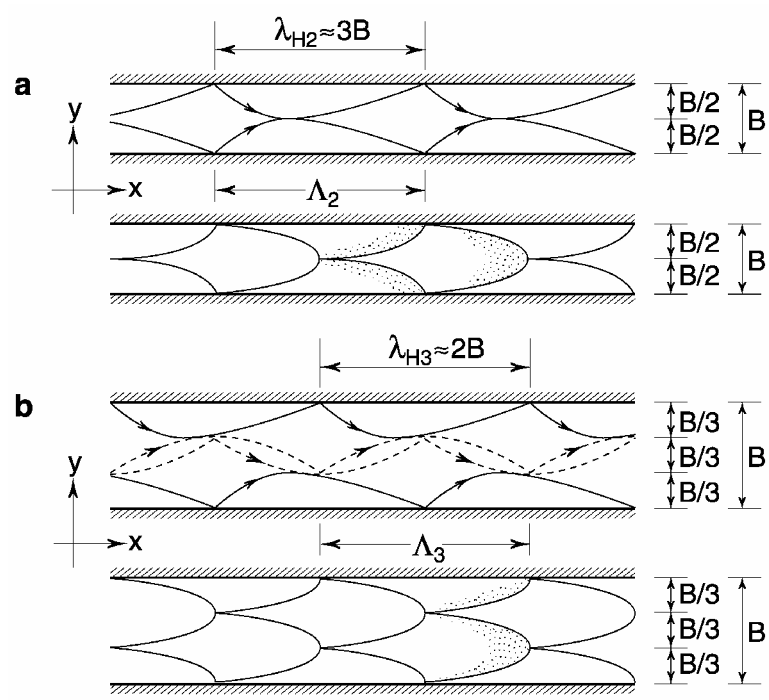

Figure 6 Two and three-row burst configurations and related bed forms (after Yalin and da Silva 2001)

i) *Plan shape of a regular meandering stream*

Following Langbein and Leopold (1966), Leopold and Langbein (1966), it appears to have become generally accepted that the centerline of an idealized, regular meandering stream can be represented best by the sine-generated function

$$\theta = \theta_0 \cos\left(2\pi \frac{l_c}{L}\right), \tag{8}$$

where θ_0 and θ are the deflection angles at $l_c = 0$ and at any l_c, respectively (Figure 7).

It can be shown (see da Silva 1991, Yalin 1992, Yalin and da Silva 2001) that in the case of a sine-generated stream, the meander length L and the meander wavelength Λ_M (see Figure 7) are interrelated by θ_0 alone:

$$\frac{L}{\Lambda_M} = \frac{1}{J_0(\theta_0)} \quad [= \sigma \text{ (sinuosity)} = S_v/S] \tag{9}$$

Here $J_0(\theta_0)$ is the Bessel function of the first kind and zero-th order of θ_0. Its graph is shown in Figure 8(a). Observe that when $\theta_0 \approx 138^\circ$, then $J_0(\theta_0) = 0$ and $L; \sigma \to \infty$. However, this can never occur, for when θ_0 reaches the value $\approx 126^\circ$ the meander loops come into contact with each other (Figure 8(b)) and the meandering flow pattern is destroyed. Hence $\theta_0 \approx 126^\circ$ gives the largest practically possible sinuosity of sine-generated channels, viz $\sigma \approx 8.5$. Note also that $\sigma = S_v/S$, where S_v is the valley slope, and S is the stream slope.

For practical purposes, $J_0(\theta_0)$ (in eq. 9) can be approximated by the following polynomial, where θ_0 is in radians:

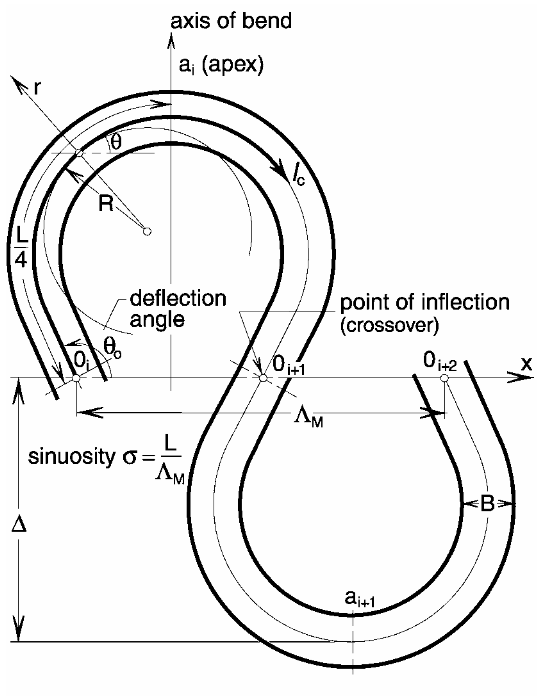

Figure 7 Schematical representation of a regular meandering stream

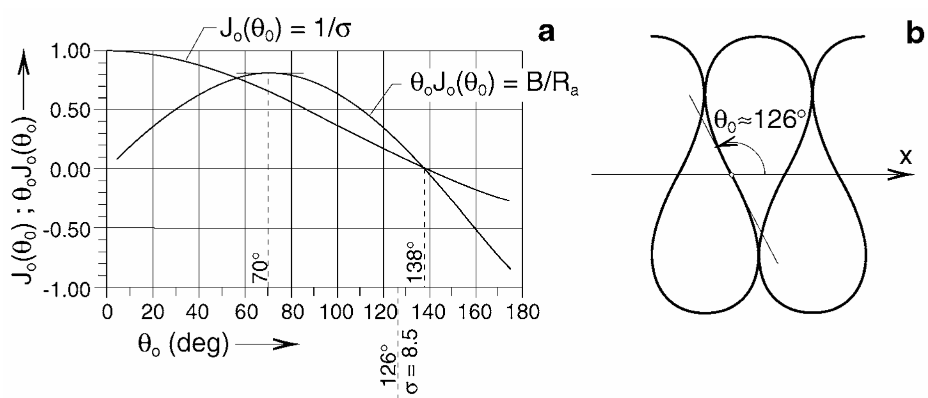

Figure 8 (a) Plot of $1/\sigma = J_0(\theta_0)$ versus θ_0; (b) Largest possible value of θ_0

$$J_0(\theta_0) \approx 1 - 2.2499997(\theta_0/3)^2 + 1.2656208(\theta_0/3)^4 - 0.3163866(\theta_0/3)^6 + \\ + 0.0444479(\theta_0/3)^8 - 0.0039444(\theta_0/3)^{10} + 0.0002100(\theta_0/3)^{12}. \qquad (10)$$

ii) *Meander wavelength*

Figure 9 shows the meander wavelength data plotted versus flow width *B*. As can be seen from this graph, the average meander wavelength Λ_M of meanders is given by

$$\Lambda_M \approx 6B. \qquad (11)$$

Observe that Figure 9 contains data not only from alluvial streams, but also from meltwater channels on ice and meanders on the Gulf Stream. These data are from Leopold et al. (1964), who appear to have been the first to realize that “the meander pattern of meltwater channels on the surface of glaciers have nearly identical geometry to the meander bends in rivers” and that “the geometry in plan view of meanders in the Gulf Stream is also similar to that of rivers”. It should be noted that, as pointed out by Leopold et al. (1964), p. 302, the “meandering channels on ice are formed without any sediment load or point-bar construction by sediment deposition” and that the meanders on the Gulf Stream too occur “… without debris load and, in this instance, without confining banks”.

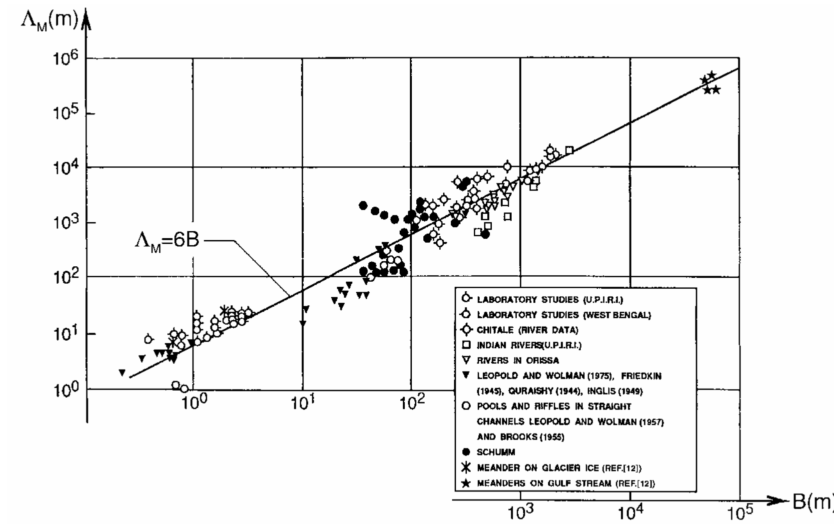

Figure 9 Plot of Λ_M versus B (after Garde and Raju 1977)

4.2 Meandering and Horizontal Bursts

From the previous sections, it should be clear that the meander wavelength Λ_M, the length of alternate bars Λ_a, and the length λ_H of horizontal bursts having the basic arrangement $n=1$ are all related to the flow width B by the same proportionality factor (≈ 6), i.e.

$$\Lambda_M \equiv \Lambda_a \equiv \lambda_H \qquad (\approx 6B)\,. \tag{12}$$

The remarkable coincidence between the (average) horizontal burst length λ_H, the (average) alternate bar length Λ_a, and the (average) meander wavelength Λ_M implied by eq. 12 suggests that both alternate bars and meanders initiate because of the same mechanism, namely horizontal bursts. Alternate bars are due to the action of horizontal bursts on the deformeable surface of the movable bed, the initiation of meandering being due to the action of horizontal bursts on the deformeable banks. The action of horizontal bursts on the banks may be by their direct impact on the banks and/or by the convective action of the internal meandering they generate. In the following, the conditions under which horizontal bursts may lead to meandering and/or to alternate bars are discussed.

The structure of the large-scale turbulence does not depend on the fluid viscosity ν. And therefore, the structure of the large-scale horizontal turbulence of a flow in a wide trapezoidal open-channel (having a flat rigid bed covered by the granular roughness $k_s \approx 2D$, where D is the average grain size) is determined solely by the ratios

$$\frac{B}{h} \quad \text{and} \quad \frac{h}{k_s} \quad \left(\sim \frac{h}{D}\right) \tag{13}$$

Clearly, these variables are applicable also to the case of a mobile bed - as long as this bed is flat and the suspended-load is not extensive.

Since the configuration of horizontal bursts is an aspect of the structure of flow past the initial bed, the number n of horizontal burst-rows must be a certain function of the variables (13):

$$n = \varphi_n\left(\frac{B}{h}, \frac{h}{D}\right) \tag{14}$$

Hence it would be only appropriate to locate the existence regions of various types of alluvial forms due to horizontal turbulence, and in particular, alternate bars and meanders on the $(B/h; h/D)$-plane. Accordingly, the B/h- and h/D-values of all the available to the authors' field and laboratory data are plotted in Figure 10. [The References to the data in this figure are given in Yalin and da Silva 2001, at the end of Chapters 2 and 4.] This plot includes alternate bars (points A), multiple bars (points C), meandering streams (M and m) and braiding streams (B and b). The scatter is gross, and the "diffusion" of points from one region to another is substantial. Nonetheless, one can still clearly identify distinct existence regions for the different types of alluvial forms, as sketched in the insert in Figure 10. The existence region of alternate bars (points A) is the region between the lines $\mathcal{L}$ and $\mathcal{L}_A$; the existence region of meanders (M, m) is the region between the lines $\mathcal{L}$ and $\mathcal{L}_M$. Clearly, the regions of alternate bars and meanders, though overlapping, are not congruent: the meandering points (M,m) extend more downwards and to the right than the points A (which, on the other hand, extend more to the left than the points (M,m)). Observe also that the line $\mathcal{L}$ appears as the common upper boundary for both A and M;m.

Figure 10 suggests the following:

i. If B/h is small (smaller than the ordinates of the line $\mathcal{L}_A$), then the horizontal burst-forming coherent structures grow until their lateral extent becomes as large as B without rubbing the bed (like in Figure 11(b)), and therefore they cannot produce "their" bed forms, viz alternate bars. Yet, the sequence of these structures can still initiate meandering by their direct impact on the banks, and/or by the convective action of the internal meandering they generate. Thus the horizontal bursts can "imprint" on the channels banks the length $\lambda_H \approx 6B_0$, *without* alternate bars. This occurs in the zone between the lines $\mathcal{L}_A$ and $\mathcal{L}_M$. Figure 12(a) shows how the sequence of horizontal bursts of an initial channel causes the flow and the alluvial banks to deform (in plan view) in a wave-like manner.

ii. If B/h is larger than the ordinates of $\mathcal{L}_A$, but smaller than those of $\mathcal{L}$, then the horizontal coherent structures are rubbing the bed (like in Figure 11(c)), and they produce first the alternate bars (as shown in Figure 5), which, acting as "guide-vanes", facilitate (accelerate) the bank deformation described in item (i) above. In this case, the points A and M can be present in the same zone (viz between the lines $\mathcal{L}$ and $\mathcal{L}_A$).

The fact that meanders can be present when alternate bars are not present (all points M in Figure 10 which are below the lower limit $\mathcal{L}_A$ of the alternate bar region) is a sufficient indication that, in contrast to what has been suggested in several earlier works (Ackers and Charlton 1970, Kinoshita 1961, Sukegawa 1970, etc.), alternate bars are not the cause of meanders. Rather, alternate bars are merely the "catalysts" which accelerate the formation of meanders which would take place even without them: the "prime mover" of the periodic bed and bank deformation of the length $\approx 6B$ is the sequence of horizontal bursts.

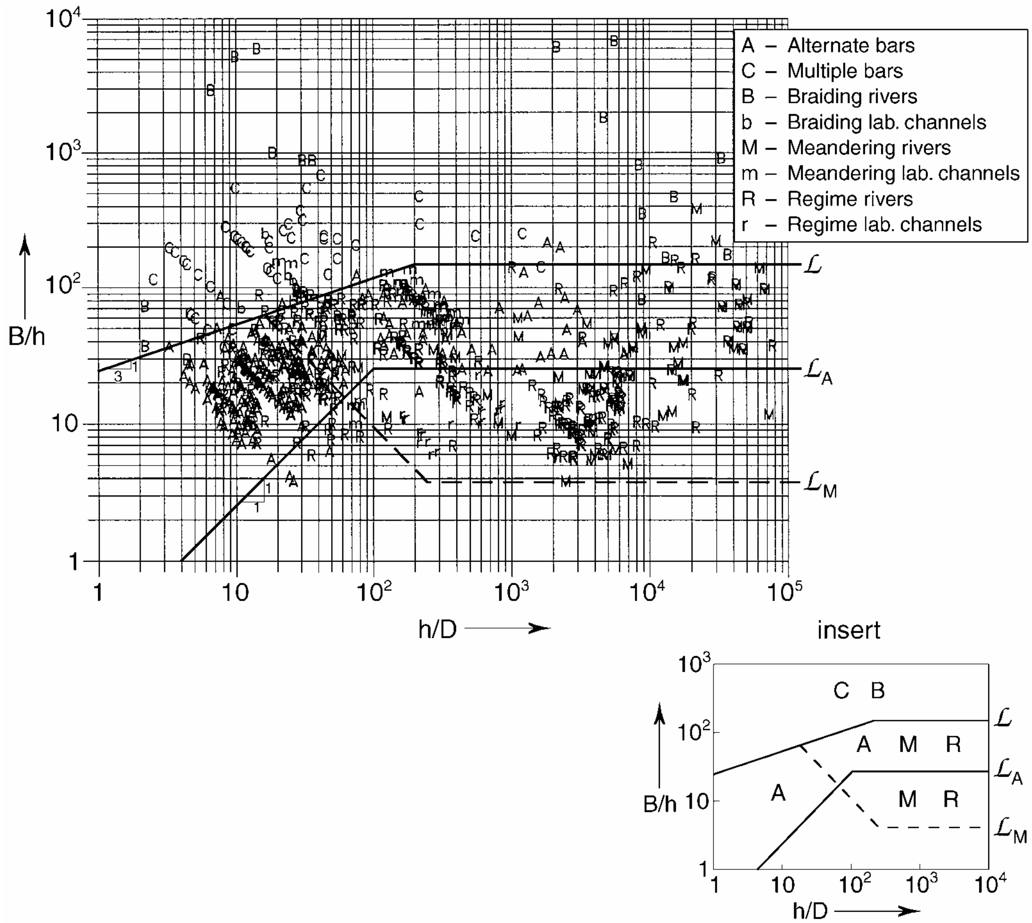

Figure 10 Existence regions of alluvial bed and plan forms on the $(B/h; h/D)$ -plane (from Yalin and da Silva 2001)

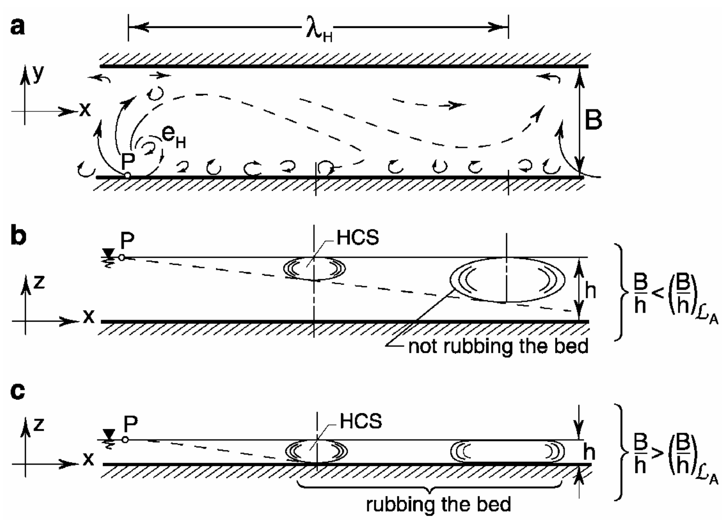

Figure 11 Evolution of a HCS. (a) Plan view; (b) and (c) Longitudinal views, corresponding to the cases where the HCS is not rubbing the bed and is rubbing the bed, respectively

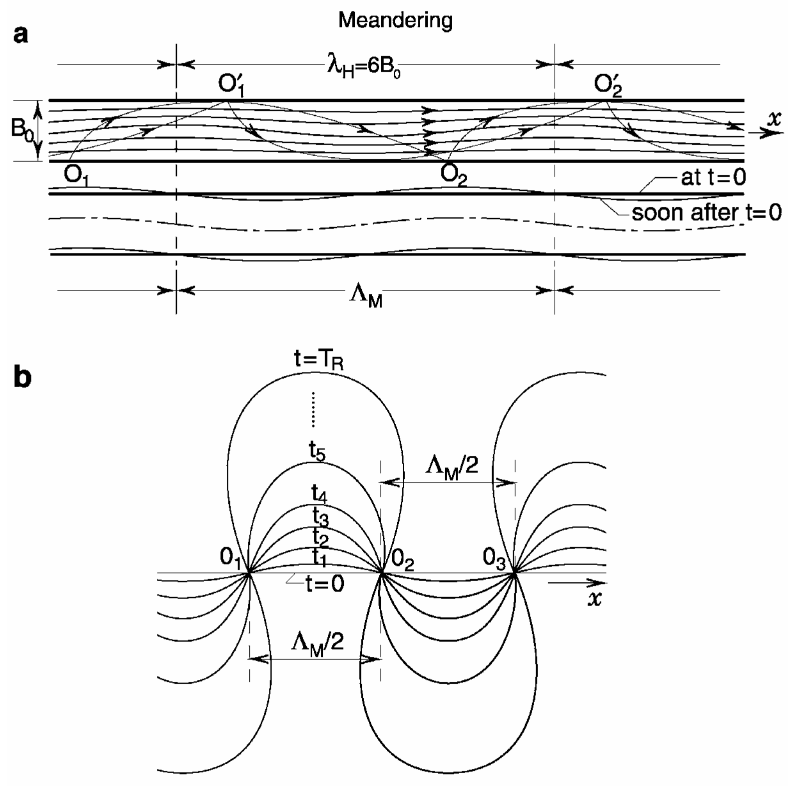

Figure 12 Initiation of meandering by horizontal turbulence and subsequent development of meanders due to the regime-trend

5. REGIME DEVELOPMENT AND TIME GROWTH OF MEANDER LOOPS

Once meandering is initiated (by large-scale horizontal turbulence), why is the subsequent process of loop expansion carried out to different degrees by different streams? The explanation for this appears to rest entirely on the regime-trend.

Regime (or stable) channels and meandering have classically been regarded and treated as independent fluvial phenomena. Bettess and White (1983) and Chang (1988) appear to have been the first to realize that the phenomena mentioned may not really be independent. Following these works, an outline of the time-growth of meander loops in the light of the regime-trend was developed by da Silva (1991), Yalin (1992) and Yalin and da Silva (2001), as summarized below.

i) Consider an experiment which starts at $t = 0$ in a straight initial channel excavated in an alluvial valley. The slope S_0 of the initial channel is the same as the valley slope S_v, i.e. $S_0 = S_v$. It is assumed that the granular material and fluid are specified, that the flow rate Q is given ($Q = Q_{bf} = const$, Q_{bf} being the bankfull flow rate), and that the conditions are such that sediment can be transported. It is also assumed that the initial channel (B_0, h_0, S_0) is such that the formation of the regime channel (B_R, h_R, S_R) is possible. The duration of formation of the regime channel is T_R.

The laboratory research (see e.g. Ackers 1964, Leopold and Wolman 1957) indicates that the variation of the flow width B, the flow depth h, and the slope S during T_R takes place as shown in the schematic Figure 13. In the (very short) part $\hat{T}_0$ of T_R, B and h vary substantially, while S remains nearly constant $(S \approx S_0)$; no regime development as such takes place. The part $\check{T}_0$ of T_R is merely the duration needed to alter (the arbitrary) B_0 and h_0 into such $\hat{B}_0$ ($\approx B_R$) and $\hat{h}_0$, say, which are in equilibrium with the existing $S \approx S_0$ and which together with S_0 are able to convey the given flow rate Q. The regime development in the proper sense takes place only after the *adjustment period* $\hat{T}_0$. (The time $t = 0$ in the previous section (see Figure 12) is to be identified with the present $t = \hat{T}_0$; therefore B_0 in Figure 12 is to be viewed as $\hat{B}_0 \approx B_R$).

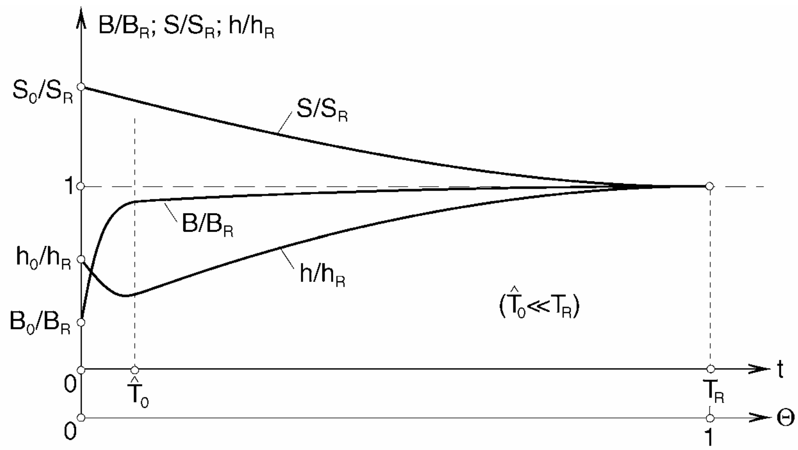

Figure 13 Regime development of flow width *B*, flow depth *h* and slope *S* (from Yalin and da Silva 2001)

According to the contemporary rational approaches to regime, the regime development is a process in which the stream appropriately alters its channel so that a certain energy-related quantity, A_* say, may be minimized. Although different authors proposed different quantities as A_* (e.g. according to Chang 1988, $A_* = \gamma QS$; according to Yang et al. 1981, $A_* = u_{av}S$; according to Jia 1990 and Yalin 1992, $A_* = Fr$, where $Fr \sim S$; according to Yalin and da Silva 2001, $A_* = u_{av}$), almost invariably A_* is such that its minimization can only be achieved through the decrement of the slope. This is in agreement with the aforementioned experimental observations.

Clearly, the decrement of the slope (from S_0 to S_R) can only be realized either by degradation (Figure 14(a)), or by meandering (for the expansion of meander loops (see Figure 14(b)), i.e. the increment of their length, means the decrement of the channel slope) – or by a combination of both. The development stops, and thus the expansion of meander loops stops, at $t = T_R$ when $S = S_R$ (see also Figure 12(b)).

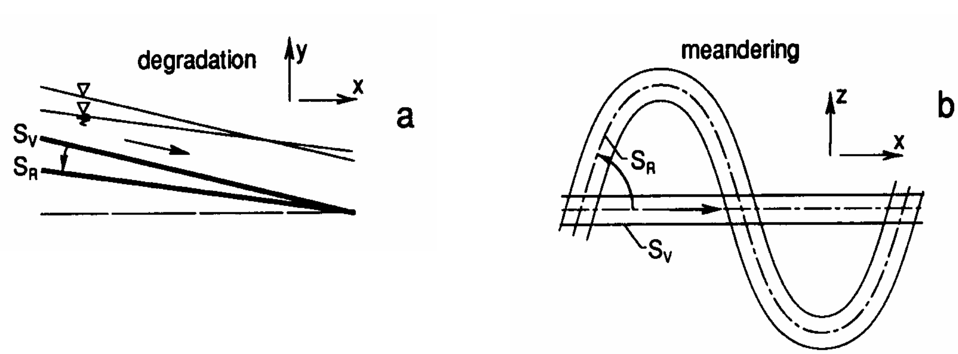

Figure 14 Regime development by degradation and meandering ($S_v > S_R$)

ii) From the explanations above, it follows that a straight channel will develop into a meandering channel only if its slope S_v is larger than the regime slope S_R, i.e. if $S_v > S_R$. Since the valley slope S_v is arbitrary, the fulfillment of the inequality $S_v > S_R$, or to that matter of $S_v < S_R$ which can be taken as the "criterion for an initial channel to remain straight" is, in a sense, a matter of chance.

If the (positive) difference $(S_v - S_R)$ is "small", then an insignificant growth of the meander amplitude Δ (see Figure 7) is sufficient to make the river slope S to be equal to S_R and the developed (stable) meandering channel is of the "moderate amplitude" type ("small" sinuosity). Conversely, if the difference $(S_v - S_R)$ is "large", then the developed (stable) meandering channel is of the "large" amplitude" type ("large" sinuosity). Finally, if $(S_v - S_R)$ is very excessive, the equality $S = S_R$ may never be achieved, for already when the channel length L is grown to a length L_1 and thus the channel slope S is reduced to a value S_1 $(< S_R)$, the corresponding deflection angle $(\theta_0)_1$ will become as large as to render the neighbouring loops to come in contact with each other – in which case the meandering pattern is destroyed and the process starts all over again. In this case, therefore, the river is never settled (for its slope is always larger than the "desired" slope S_R). Such a river is destined to exist in the dynamic state – "try and try again" forever. The Mississippi River is one of the best known examples of this type of river.

6. CONCLUDING REMARKS

From the study of alluvial forms in the light of the recent discoveries in turbulence, it is concluded that the formation of bars and meanders is explained best by means of horizontal turbulence. The large-scale structures of horizontal turbulence initiate meandering and they provide it with its linear scale. The regime trend ensures that the so-initiated meandering continues to develop (grow in time): the development terminates when the regime state is achieved.

From the content of this paper, it follows that an initially straight stream in a cohesionless alluvium can meander only if it satisfies the following conditions:

1- it transports the sediment (so that its boundaries can deform);
2- it conveys a turbulent flow (otherwise there will be no bursts to initiate the periodic bank deformation of the wavelength $\Lambda_M \equiv \lambda_H \approx 6B$);
3- its slope is larger than the regime slope (otherwise the stream will not endeavour to reduce its slope by increasing its length, which brings the sinuosity σ into being);
4- its initial values of B/h and h/D (at time $t = \hat{T}_0$, when the stream is still straight) must be such that the initial point $\hat{P}_0$ is in the meander region of the $(B/h; h/D)$-plane in Figure 10 (otherwise the horizontal burst sequences will not be of the type needed to deform the banks in the anti-symmetrical and periodic (along x) manner).

The totality of these conditions 1 to 4 forms the set of the *necessary* and *sufficient* conditions for an alluvial stream to meander.

Assuming that the conditions above are met, then knowing the values of the bankfull flow rate Q_{bf}, grain properties, and the initial (or valley) slope S_0, the regime (or stable) meandering channel centerline – provided the stream will develop entirely by meandering – can be calculated as follows:

1- Knowing Q_{bf} and the grain properties, compute (with the aid of a regime method) the values of the regime channel characteristics B_R and S_R;
2- Compute $\sigma_R = S_0 / S_R$;
3- Determine $(\theta_0)_R$ from eq. 9, viz $\sigma_R = 1/J_0((\theta_0)_R)$, where $J_0((\theta_0)_R)$ can be computed with the aid of eq. 10.
4- Determine the coordinates of the channel centerline with the aid of eq. 8.

REFERENCES

Ackers, P. and Charlton, F.G. (1970). “The Geometry of Small Meandering Streams”, Proc. Instn. Civ. Engineers, Paper 73286S, London.

Ackers, P. (1964). “Experiments on Small Streams in alluvium”, J. Hydr. Div. ASCE, Vol. 90, No. HY4.

Bettess, R. and White, W.R. (1983). “Meandering and Braiding of Alluvial Channels”, Proc. Instn. Civ. Engrs., Part 2, 75, Sept.

Blackwelder, R.F. (1978). “The Bursting Process in Turbulent Boundary Layers”, Lehigh Workshop on Coherent Structures in Turbulent Boundary Layers.

Cantwell, B.J. (1981). “Organised Motion in Turbulent Flow”, Ann. Rev. Fluid Mech, Vol. 13.

Chang, H.H. (1988). Fluvial Processes in River Engineering, John Wiley and Sons.

da Silva, A.M.F. (1991). Alternate Bars and Related Alluvial Processes, M.Sc. Thesis, Dept. of Civil Engrg., Queen's Univ., Kingston, Canada.

Dementiev, M.A. (1962). Investigation of Flow Velocity Fluctuations and Their Influences on the Flow Rate of Mountainous Rivers, (In Russian) Tech. Report of the State Hydro-Geological Inst. (GGI), Vol. 98.

Fujita, Y. and Muramoto, Y. (1989). “Multiple Bars and Stream Braiding”, Int. Conf. on River Regime, W.R. White ed., John Wiley and Sons.

Gad-el-Hak, M. and Hussain, A.K.M.F. (1986). “Coherent Structures in a Turbulent Boundary Layer”, Phys. Fluids, Vol. 29, July.

Garde, R.J. and Raju, K.G.R. (1977). Mechanics of Sediment Transportation and Alluvial Stream Problems, Wiley Eastern, New Dehli.

Grishanin, K.V. (1979). Dynamics of Alluvial Streams, Gidrometeoizdat, Leningrad.

Hayashi, T. (1971). “Study of the cause of meanders”, Trans. JSCE, Vol. 2, Part 2.

Hussain, A.K.M.F. (1983). “Coherent Structures – Reality and Myth”, Phys. Fluids, Vol. 26, Oct.

Ikeda, S. (1984). “Prediction of Alternate Bar Wavelength and Height”, J. Hydr. Engrg., ASCE, Vol. 110, No. 4, April.

Ikeda, H. (1983). Experiments on Bed Load Transport, Bed Forms and Sedimentary Structures Using Fine gravel in the 4-Meter-Wide Flume”, Environmental Research Center Papers, No. 2, The University of Tsukuba.

Jackson, G. (1976). “Sedimentological and Fluid-Dynamic Implications of the Turbulent Bursting Phenomenon in Geophysical Flows”, J. Fluid Mech., Vol. 77, 531-560.

Jaeggi, M. (1984). “Formation and Effects of Alternate Bars”, J. Hydr. Engrg., ASCE, Vol. 110, No. 2.

Jia, Y. (1990). “Minimum Froude Number and the Equilibrium of Alluvial Sand Rivers”, Earth Surf. Processes and Landforms, Vol. 15.

JSCE Task Committee on the Bed Configuration and Hydraulic Resistance of Alluvial Streams (1973). “The Bed Configuration and Roughness of Alluvial Streams”, (In Japanese) Proc. JSCE, No. 210, Feb.

Kinoshita, R. (1961). “Investigation of the Channel Deformation of the Ishikari River”, (In Japanese) Science and Technology Agency, Bureau of Resources, Memorandum No. 36.

Kishi, T. (1980). “Bed Forms and Hydraulic Relations for Alluvial Streams”, Application of Stochastic Processes in Sediment Transport, H.W. Shen and K. Kikkawa eds., Water Resources Publications, Litleton, Colo.

Klaven, A.B. (1966). “Investigation of Structure of Turbulent Streams”, Tech. Report of the State Hydro-Geological Inst. (GGI), Vol. 136.

Kondratiev, N., Popov, I. and Snishchenko, B. 1982. Foundations of Hydromorphological Theory of Fluvial Processes, (In Russian) Gidrometeoizdat, Leningrad.

Langbein, W.B. and Leopold, L.B. (1966). “River Meanders – Theory of Minimum Variance”. U.S. Geol. Survey Prof. Paper 422-H.
Leopold, L.B. and Langbein, W.B. (1966). “River Meanders”. Sci. Am., 214.
Leopold, L.B., Wolman, M.G. and Miller, J.P. (1964). Fluvial Processes in Geomorphology, W.H. Freeman, San Francisco.
Leopold, L.B. and Wolman, M.G. (1957). “River Channel Patterns: Braided, Meandering and Straight”, U.S. Geol. Survey Professional Paper 282-B.
Matthes, G.H. (1947). “Macroturbulence in Natural Stream Flow”, Trans. Am. Geophys. Union, Vol. 28, No. 2.
Muramoto, Y. and Fujita, Y. (1978). “The Configuration of Meso-Scale River Bed Configuration and the Criteria of its Formation, 2nd Meeting of Hydr. Res. in Japan.
Nezu, I. and Nakagawa, H. (1993). Turbulence in Open-Channel Flows, IAHR Monograph, A.A. Balkema, Rotterdam, The Netherlands.
Rashidi, M. and Banerjee, S. (1988). “Turbulence Structure in Free-Surface Channel Flows”, Phys. Fluids, Vol. 31, Sept.
Roy, A.G., Buffin-Bélanger, T., Lamarre, H. and Kirkbride, A.D. (2004). “Size, Shape and Dynamics of Large-Scale Turbulent Flow Structures in a Gravel-Bed River”, J. Fluid Mech., Vol. 500, 1-27.
Sukegawa, N. (1970). “Condition for the Occurrence of River Meanders”, J. Faculty Engrg., Tokyo Univ., Vol. 30.
Tison, L.J. (1949). “Origine des Ondes de Sable et des Bancs de Sable Sous l’Action des Courants”, Report II-13, 3rd Congress IAHR, Grenoble, France.
Velikanov, M.A. (1958). Alluvial Processes: Fundamental Principles, State Publishing House for Physico-Mathematical Literature, Moscow.
Velikanov, M.A. (1955). Dynamics of Aluvial Streams, Vol. II, Sediment and Bed Flow, State Publishing House for Theoretical and Technical Literature, Moscow.
Yalin, M.S. and da Silva, A.M.F. (2001). Fluvial Processes, IAHR Monograph, IAHR, Delft, The Netherlands.
Yalin, M.S. (1992). River Mechanics, Pergamon Press, Oxford.
Yalin, M.S. (1977). Mechanics of Sediment Transport, Pergamon Press, Oxford.
Yang, C.T., Song, C.C.S. and Woldenberg, M.J. (1981). “Hydraulic Geometry and Mnimum Rate of Energy Dissipation”, Water Resour. Res., 17.
Yokosi, S. (1967). “The Structure of River Turbulence”, Bull. Disaster Prevention Res. Inst., Kyoto Univ., Vol. 17, Part 2, No. 121, Oct.

LIST OF SYMBOLS

A_*	energy-related property of flow (subjected to minimization during the regime channel formation)
c	flow friction factor $(= u_{av} / v_*)$
B	flow width
D	typical grain size (usually D_{50})
Fr	flow Froude number $(= u_{av} / \sqrt{g h_{av}})$
h	flow depth
$J_0(\theta_0)$	Bessel function of first kind and zero-th order (of θ_0)
k_s	granular roughness of bed surface $(k_s \approx 2D_{50})$
L	meander length (measured along l_c)

l_c	longitudinal coordinate along the centreline of a meandering flow; $l_c = 0$ at the crossover O_i (see Figure 7)
n	number of horizontal-burst rows
Q	flow rate
Re	flow Reynolds number $(= h u_{av} / \nu)$
S	bed slope
S_v	valley slope
t	time
T_V, T_H	development duration of vertical and horizontal bursts, respectively
T_R	development duration of the regime channel
u_{av}	channel-averaged flow velocity
v_*	shear velocity $(= \sqrt{\tau_0 / \rho})$
x	direction of rectilinear flow; also general direction of meandering flow
y	direction horizontally perpendicular to x
z	vertical direction
$\phi_d(X, Z)$	function of the grain size Reynolds number $X = v_* D / \nu$ and the relative flow depth $Z = h / D$
γ	fluid specific weight
θ, θ_0	deflection angle of a meandering flow at any l_c and at $l_c = 0$, respectively (see Figure 7)
λ_V, λ_H	length of vertical and horizontal bursts, respectively
Λ_i	length of bed form i ($i = d$ if dunes; $i = a$ if alternate bars)
Λ_M	meander wavelength
ν	fluid kinematic viscosity
ρ	fluid density
σ	sinuosity of a meandering flow ($\sigma = L / \Lambda_M$)

Subscripts:

0	marks the value of a quantity at time $t = 0$
R	marks the regime value of a quantity